Opto-Electronic Advances

Supplementary information

2021, Vol. 4, No. 12

DOI: 10.29026/oea.2021.200101

Plasmon-enhanced nanosoldering of silver nanoparticles for high-conductive nanowires electrodes

Yuan-Yuan Zhao[1†], Xue-Liang Ren[2†], Mei-Ling Zheng[2,3*], Feng Jin[2], Jie Liu[2], Xian-Zi Dong[2], Zhen-Sheng Zhao[2] and Xuan-Ming Duan[1*]

[1]Guangdong Provincial Key Laboratory of Optical Fiber Sensing and Communications, Institute of Photonics Technology, Jinan University, Guangzhou 511443, China; [2]Laboratory of Organic NanoPhotonics and CAS Key Laboratory of Bio-Inspired Materials and Interfacial Science, Technical Institute of Physics and Chemistry, Chinese Academy of Sciences, Beijing 100190, China; [3]School of Future Technologies, University of Chinese Academy of Sciences, Yanqihu Campus, Beijing 101407, China.

[†]These authors contributed equally to this work.

[*]Correspondence: ML Zheng, E-mail: zhengmeiling@mail.ipc.ac.cn; XM Duan, E-mail: xmduan@jnu.edu.cn

This file includes:

Supplementary information for this paper is available at https://doi.org/10.29026/oea.2021.200101

Section 1: Measurement of the resistance of Ag NWs

Figure S1 shows a process of a measurement for the resistance using two-terminal method[1–3]. In this study, specific process is shown as follows: The Ag NWs were fabricated on the glass substrate by FsLDW (**Step 1**)[4], then the Ag NWs were coated by a copper mesh (line width of 50 μm) to form a 50 μm-wide isolated channel (**Step 2**). After evaporating the Ag films electrode, the electrical contact pads with a size of 500 μm × 500 μm were evaporated on two opposite sides of the Ag NWs to allow for the electrical characterization (**Step 3** and **Step 4**).

The electrical resistance of the Ag NWs was measured by a two-probe setup in Fig. S1(b), because the sum of the contact resistance and electrode resistance (~3 Ω in this work) can be ignored[1]. Two probes were positioned on each electrical contact pad, and *I*-*V* curves were measured by scanning the voltage over the Ag NWs from −0.1 V to 0.1 V and measuring the current through the Ag NWs. We have calculated the resistance value of our fabricated Ag NWs electrode according to the equation $R=V/I$.

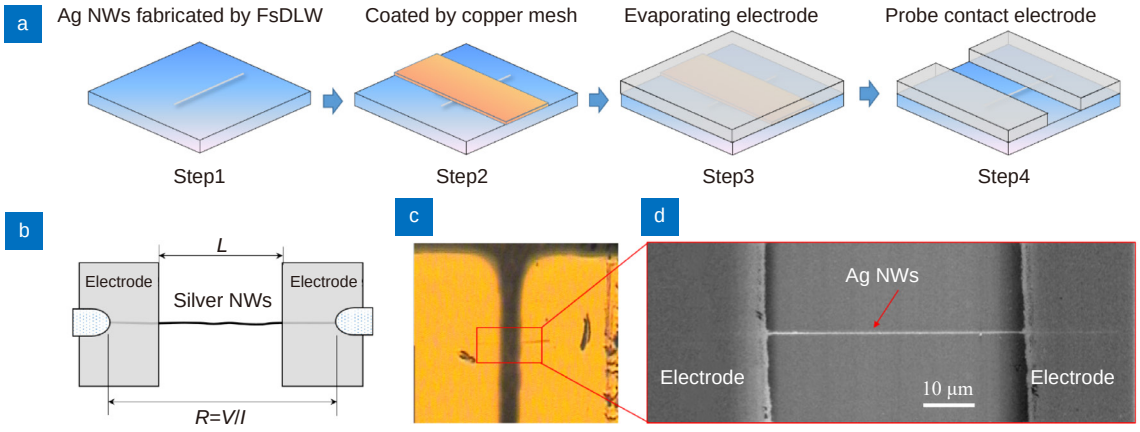

Fig. S1 | (**a**) Flow diagram of measuring resistance value *R* of Ag NWs. (**b**) Schematic of two-probe measurement of resistance. (**c**) Real-time image of the measurement process. (**d**) SEM image of the Ag NWs evaporated by electrical contact pads.

Section 2: Morphologies of Ag NWs produced from Ag ion solution at different concentrations of proline

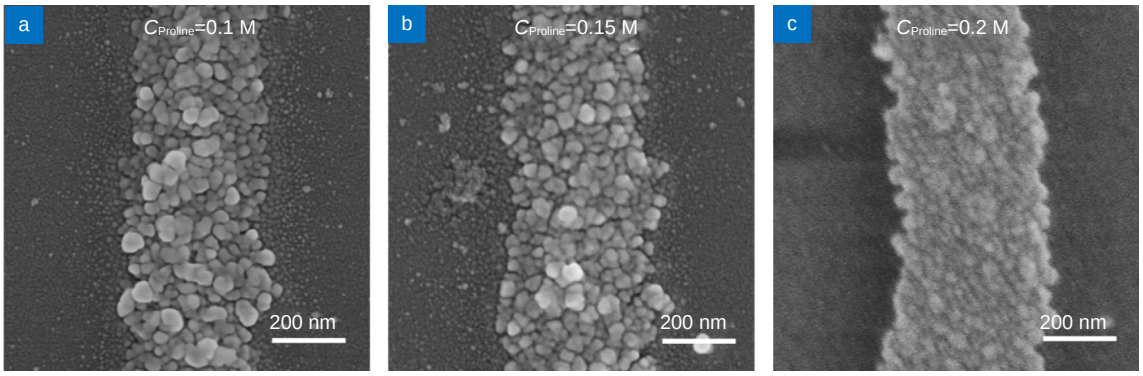

Fig. S2 | Morphologies of Ag NWs produced from Ag ion solution at the concentrations of proline of (**a**) 0.1 M, (**b**) 0.15 M and (**c**) 0.2 M.

Section 3: The measured *I-V* curves of Ag NWs electrodes irradiated at different laser power densities

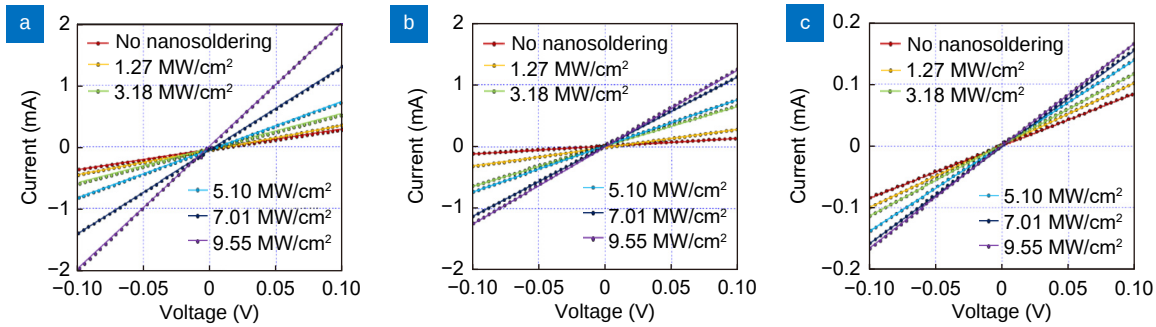

Fig. S3 | Measured *I-V* curves of Ag NWs electrodes including Ag NPs at different diameters of (**a**) 30 nm, (**b**) 28 nm, and (**c**) 15 nm.

Section 4: The measured *I-V* curves of Ag NWs electrodes irradiated at different nanosoldering time

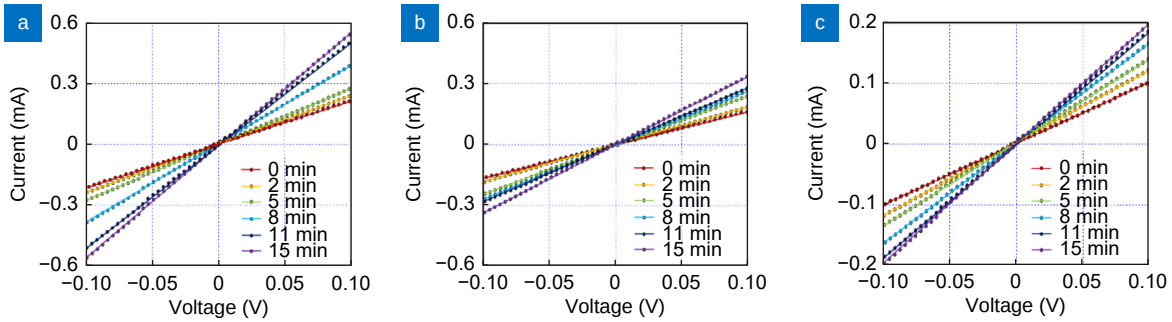

Fig. S4 | Measured *I-V* curves of Ag NWs electrodes including Ag NPs at different diameters of (**a**) 30 nm, (**b**) 28 nm, and (**c**) 15 nm.

Section 5: The melting point versus the diameter of Ag NPs

Theoretical consideration about the size effect on the melting point suggests that the melting temperature of Ag NPs is found to be size-dependent and significantly lower than that for bulk material[5]. The decrease of the melting point ΔT for small NPs of radius r can be calculated from the Gibbs-Thomson equation[6]:

$$\Delta T = \frac{4\sigma M T_{\mathrm{m}}}{\Delta H_{\mathrm{m}} r \rho}, \tag{1}$$

where σ= 1.02 J/m² is the surface energy, M= 107.9 g/mol is the molar mass, T_{m}=1233 K is the melting point of the bulk Ag, ΔH_{m}=11.3 kJ/mol is the melting enthalpy and ρ=10.5 g/cm³ is the density of Ag.

The melting point dependency on the diameter of Ag NPs is obtained as shown in Fig. S4. Compared to the bulk material of Ag (T_{m}=1233 K), the melting point of Ag NPs with the size of 8 nm (the smallest NPs were obtained in our experiment, as shown in Fig. 5(a)) can be reduced to 0.2 T_{m} (Fig. S5). Here are two special cases: (i) For Ag NPs with a

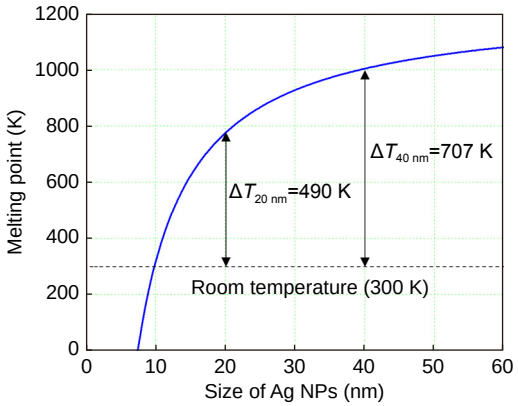

Fig. S5 | The melting point versus the diameter of Ag NPs.

particle size of 20 nm at room temperature (300 K), the required heat generation to reach the melting point is 490 K. (ii) For Ag NPs with a particle size of 40 nm at room temperature, the required heat generation to reach the melting point is 707 K.

Section 6: The calculated light field intensity at the gaps between the adjacent Ag NPs

To quantitatively evaluate the collective response of the optical field enhancement among the aggregated NPs, numerically reconstructed the NPs distribution of NWs using the statistical morphologies of the Ag NPs were studied via the FEM simulation. As shown in Fig. S6(a), simplified random distributed Ag NPs satisfy the statistical results of a 30 nm average-size, which corresponds to the Ag NWs fabricated from Ag ion solution of the concentration of proline of 0.1 M or 0.15 M.

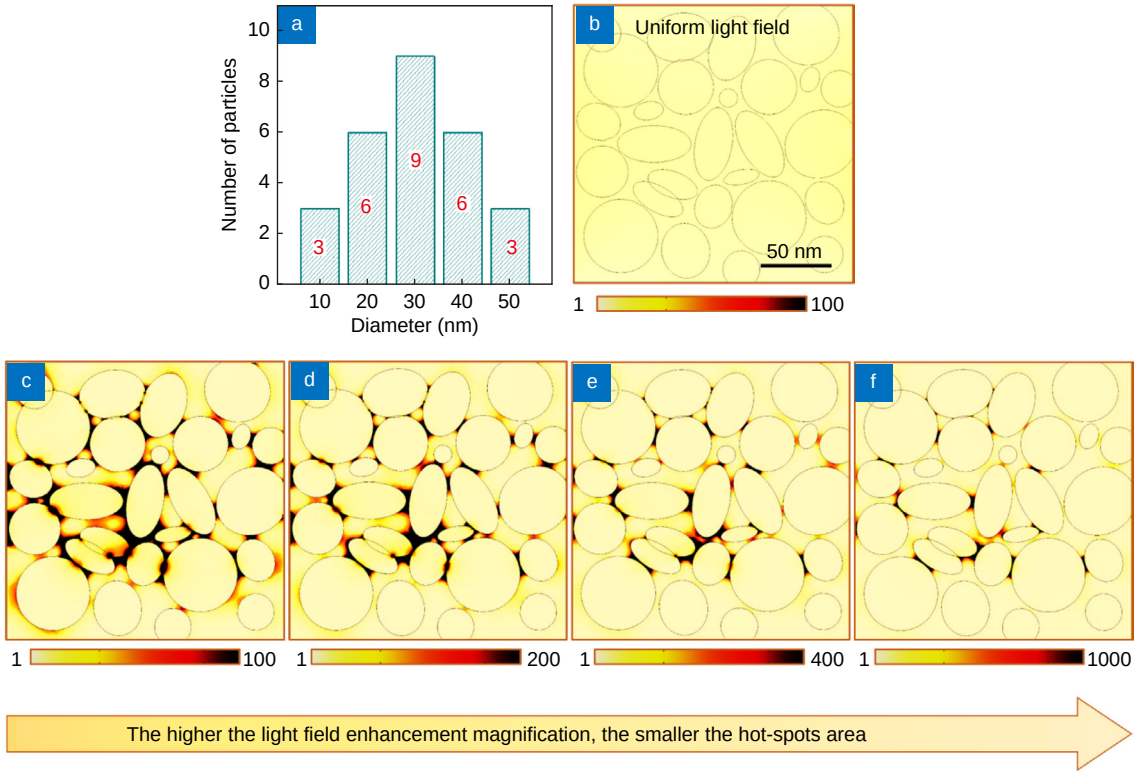

Fig. S6 | (**a**) Simplified particle size distribution similar to the case in Fig. 5(a), calculated the concentrated light field intensity. (**b**) Irrespective of surface SPP effect. (**c**–**f**) The black areas for the concentrated light field intensity increased 100, 200, 400, 1000 times.

Figure S6(b) shows that the Ag NPs under the average light field irrespective of surface plasmon resonance (SPP). When we consider the SPP in the simulation, the enhanced light field intensity in the gap increases tens even thousands of times compared to the average light field. The black areas, also named "hot-spots" express the enhanced light field intensity increases 100, 200, 400, 1000 times [Fig. S6(c–f)], respectively.

Section 7: Heat generation versus the diameter of Ag NPs and laser power density

In the steady-state regime, the local temperature around a single NP is described by the equation[7,8], and the maximum temperature increase occurs at the particle surface and is given by:

$$\Delta T_{\max}(I_0) = \frac{R_{\mathrm{NP}}^2}{3k_0}\frac{\omega}{8\pi}\left|\frac{3\varepsilon_0}{2\varepsilon_0+\varepsilon_{NP}}\right|^2 Im(\varepsilon_{\mathrm{NP}})\frac{8\pi\cdot I_0}{c\sqrt{\varepsilon_0}}, \tag{2}$$

where T is the local temperature, I_0 is the laser intensity, R is the radius of Ag NP, k_0 is the thremal conductivity of the surrouding medium, $\varepsilon_{\mathrm{NP}}$ and ε_0 are the dielectric constants of the NP and surrounding medium, respectively.

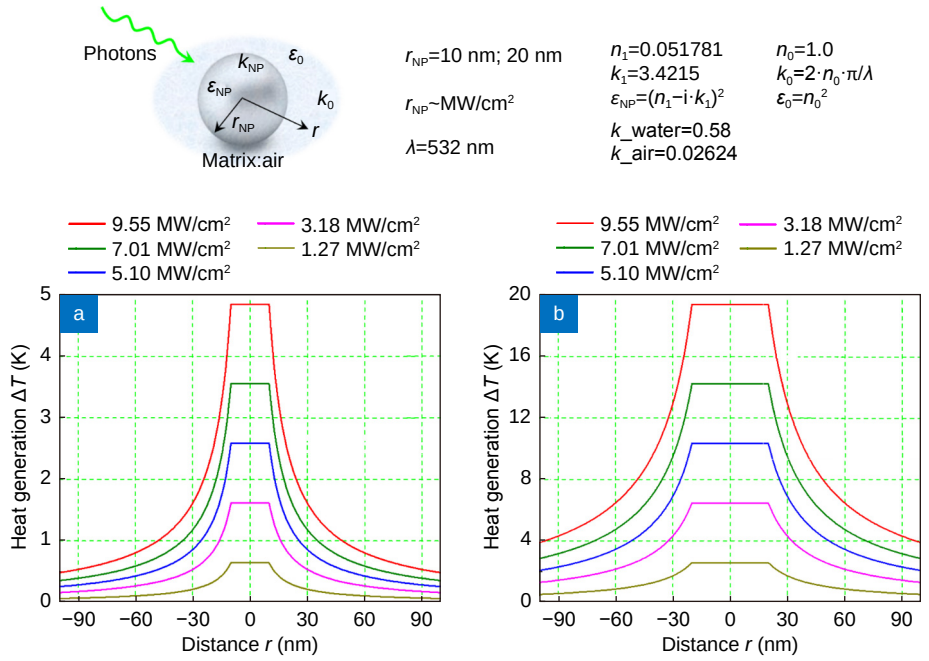

Fig. S7 | Calculated temperature increase for a single Ag NP at different diameters of (**a**) 20 nm and (**b**) 40 nm.

References

1. Zhao YY, Zheng ML, Dong XZ, Jin F, Liu J et al. Tailored silver grid as transparent electrodes directly written by femtosecond laser. *Appl Phys Lett* **108**, 221104 (2016).
2. van de Groep J, Spinelli P, Polman A. Transparent conducting silver nanowire networks. *Nano Lett* **12**, 3138–3144 (2012).
3. Hu L, Hecht DS, Grüner G. Percolation in transparent and conducting carbon nanotube networks. *Nano Lett* **4**, 2513–2517 (2004).
4. Ren XL, Zheng ML, Jin F, Zhao YY, Dong XZ et al. Laser direct writing of silver nanowire with amino acids-assisted multiphoton photoreduction. *J Phys Chem C* **120**, 26532–26538 (2016).
5. Shyjumon I, Gopinadhan M, Ivanova O, Quaas M, Wulff H et al. Structural deformation, melting point and lattice parameter studies of size selected silver clusters. *Eur Phys J D* **37**, 409–415 (2006).
6. Meyer K. *Physikalisch Chemische Kristallographie* (Deutscher Verlag für Grundstoffindustrie, Leipzig, 1968).
7. Govorov AO, Zhang W, Skeini T, Richardson H, Lee J et al. Gold nanoparticle ensembles as heaters and actuators: melting and collective plasmon resonances. *Nanoscale Res Lett* **1**, 84 (2006).
8. Govorov AO, Richardson HH. Generating heat with metal nanoparticles. *Nano Today* **2**, 30–38 (2007).